Topographic Modulation of the Orientation and Shape of Cell Nuclei and Their Influence on the Measured Elastic Modulus of Epithelial Cells

Clayton T. McKee,[†] Vijay K. Raghunathan,[†] Paul F. Nealey,[‡] Paul Russell,[†] and Christopher J. Murphy[†§*]
[†]Department of Surgical and Radiological Sciences, School of Veterinary Medicine, University of California-Davis, Davis, California; [‡]Department of Chemical and Biological Engineering, School of Engineering, University of Wisconsin-Madison, Madison, Wisconsin; and [§]Department of Ophthalmology and Vision Science, School of Medicine, University of California-Davis, Davis, California

ABSTRACT The influence of nucleus shape and orientation on the elastic modulus of epithelial cells was investigated with atomic force microscopy. The shape and orientation were controlled by presenting the epithelial cells with anisotropic parallel ridges and grooves of varying pitch at the cell substratum. As the cells oriented to the underlying topography, the volume of the nucleus increased as the pitch of the topography increased from 400 nm to 2000 nm. The increase in nucleus volume was reflected by an increase in the measured elastic modulus of the topographically aligned cells. Significant alterations in the shape of the nucleus, by intimate contact with the topographic ridge and grooves of the underlying cell, were also observed via confocal microscopy, indicating that the nucleus may also act as a direct mechanosensor of substratum topography.

INTRODUCTION

Historically, cellular behaviors have been studied on flat, rigid substrates such as glass or plastic. Cells cultured on these substrates are presented with nonphysiologic biophysical cues in the form of compliance (modulus in the gigapascal range) and topography (absent), which force cells to behave in ways that may not accurately reflect the behavior of these same cells in vivo. For example, in the absence of biochemical cues, biophysical signaling (e.g., substratum topography or compliance) can directly influence the cytoskeleton (1), and therefore the mechanics (2–4), of cells. These cues also regulate migration (5,6), proliferation (7,8), differentiation (9,10), morphology (11,12), and response to therapeutic agents (4). Reports have also shown that topographically patterned substrates can significantly alter gene expression (13), with one study (14) reporting >3000 genes being up- or downregulated by more than twofold by the presentation of topographic cues in the biomimetic scale. Thus, cells sense their extracellular environment and can modulate their structural shape and internal processes to react to changes that they sense.

The atomic force microscope (AFM) has been used to understand more fully how externally induced changes influence the dynamic internal behavior of a cell (4,15,16). However, cells are not isotropic or homogeneous in composition, and therefore, interpretation of a substrate-induced mechanical response of a cell to an indenting AFM probe is complicated by its various intracellular components (11,17,18). Two major mechanical components of a cell are the cytoskeleton and the nucleus; the mechanical properties of which are not mutually exclusive (19–24). The mechanical and structural properties of isolated and in situ cell nuclei, as well as the cell cytoskeleton as a whole, have been studied and reported on in detail (25–27). On flat tissue culture substrates, adherent cells and nuclei do not preferentially align in any particular direction. In a similar way, nonadherent cells and nuclei tend to adopt spherical shapes (inherently no orientation). Both of these situations are beneficial if the mean mechanical properties of the cell or nuclei are of interest. It remains poorly understood, however, how the orientation and shape of the cytoskeleton and nucleus affect the mechanics of the cell body as a whole. A means to control the orientation or shape of the cell cytoskeleton and nucleus would therefore be beneficial in the measurement of the mechanical properties. We have shown previously that by presenting cells with anisotropically ordered parallel ridges and grooves of varying pitch, it is possible to control the net orientation of the adherent cell cytoskeleton of endothelial, epithelial, and fibroblast cells (28–30).

Topographically responsive cells demonstrate changes in expression of cytoskeletal components, which are known to modulate the elastic modulus of cells in the absence of topographic cues (31). The nucleus, which is the largest and one of the stiffest organelles within the cell body, is directly linked to the cytoskeleton (32), and we therefore expect that changes in the cytoskeleton may regulate the mechanical properties of the nucleus. In a similar way, changes in the mechanics of the nucleus may also be reflected in the mechanical response of the cell body as a whole. In this article, we have extended our previous alignment studies to ascertain not only the orientation response of the cytoskeleton but also that of the nucleus in response to anisotropically ordered topographic cues. By altering the topographic cues, changes in cellular and nuclear orientation and shape occur and these cellular modifications have the potential to influence the elastic modulus of the cell as measured by AFM.

Submitted June 15, 2011, and accepted for publication September 26, 2011.

*Correspondence: cjmurphy@ucdavis.edu

Editor: Levi A. Gheber.

0006-3495/11/11/2139/8 $2.00

doi: 10.1016/j.bpj.2011.09.042

MATERIALS AND METHODS

Topographically patterned substrates

The topographically patterned substrates used in these studies were made from Norland Optical Adhesive 81 (NOA81). Details on substrate preparation have been described in previous publications (28,33). The topographies are defined by their pitch (ridge width + groove width) as 400, 800, 1200, 1600, and 2000 nm, all with equal ridge and groove widths and a constant depth of 300 nm. Depth of pitch is a critical aspect in cell recognition of topography (34). All of these topographies were stamped onto a single glass-bottomed petri dish (FD5040-100, World Precision Intruments, Sarasota, FL), using a single stamp, with each pitch occupying an area of 4 mm^2 (see Fig. 2 for an example of the topography). The substrates also have flat areas located between the patterned regions with an identical surface chemistry to the topographically patterned areas. We refer to these substrates as six-packs and used them for both the cell orientation and mechanics studies. All of our topographies were coated in a proprietary mixture of monomeric fibronectin and collagen (FNC coating mix, AnthenaES, Baltimore, MD) for 2 min before addition of cells. The provision of an FNC-coated surface facilitated cell adhesion.

Cell line and immunohistochemistry

Immortalized human corneal epithelial cells (HTCEpi) (35), were kindly provided by Dr. James V. Jester (University of California, Irvine) and were maintained in Epilife medium (Invitrogen, Carlsbad, CA) and plated at 60,000–80,000 cells/dish. This ensured that a significant number of adherent cells, which were not in physical contact, occupied the topographies. These cells stratify and differentiate in a fashion similar to that of primary human corneal epithelium (35). The cells were cultured overnight on six-packs at 37°C and 5% CO_2. Mechanical measurements were conducted on live cells. Cells for orientation analysis were fixed with 4% formalin in 1× PBS. The orientation of actin cytoskeleton and nuclei were obtained by imaging cells stained with phalloidin-AlexaFluor 568 (Invitrogen) and DAPI (BioGenex, San Ramon, CA), respectively.

Cytoskeleton and nucleus orientation analysis

The orientation and area analysis of the cytoskeleton and nucleus of individual cells adhered to the six-pack substrates were determined from fluorescent images analyzed with IGOR 6.2 (Wavemetrics, Lake Oswego, OR). We used IGOR to define the boundary of the cell and nucleus, determine the orientation of the cell and nucleus in relation to the underlying pitch, ensure that a particular nucleus was paired to the appropriate cell body, and, finally, compile all the results into a single file for statistical analysis. Cells included for analysis had to be fully contained within the border of the image, not in physical contact with other cells, and not undergoing mitosis. The inclusion criterion of the nucleus was dependent on cell inclusion, resulting in the same number of nuclei and cells for analysis. The orientation of the cells and nuclei was based on the angle between the major axis of the object and the long axis of the underlying topography. The major axis was based on an ellipse of the recreated cytoskeleton or nucleus, which conserved the total area of the object. We considered objects between 0° and 10° as aligned parallel and objects between 80° and 90° as aligned perpendicular to topography.

Fluorescent images for the orientation analysis were collected using an inverted fluorescent microscope (Axio Observer A1, Carl Zeiss, Thornwood, NY). For orientation analysis, six separate plates of HTCEpi cells were imaged. From each dish, four distinct 10× images were collected from each topography and flat surface, for a total of 24 images per topography. This resulted in cell counts ranging from ~250 to 400 cells for each topography. Fig. 1 shows a sample fluorescent image, the result of our boundary recreation using IGOR and examples of excluded objects. Images of cell nuclei were also collected with an FV1000 confocal microscope (Olympus, Center Valley, PA) for volume analysis.

Contact mechanics of cells

The contact mechanics of the live cells aligned by the topography were determined by probing the cells with an AFM (MFP-3D-BIO, Asylum Research, Santa Barbara, CA), as described previously (36,37). The probes used in this study were silicon nitride cantilevers with a square pyramid tip incorporated at the free end ($k = 0.06$ N/m; PNP-TR-50, Nano And More, Lady's Island, SC). Spring constants of the cantilevers were measured independently for each experiment (38). All probe indentations were performed over the central region of the cell in an area where the nucleus was present. Contact between the AFM tip and cell was defined by visually noting when the cantilever deflection deviated from a linear extrapolation of zero force. Four separate experiments were performed on each topography, with five force-versus-indentation curves measured from each of five aligned cells per pitch, for a total of 20 separate cells (indentation speed, 2 μm/s). Young's modulus of the HTCEpi cells was quantified by fitting an average force-versus-indentation curve generated from the five separate cells on each individual pitch, using Eq. 1 (39). By fitting the average of multiple force-versus-indentation curves, potential error in the interpretation of tip-cell contact was minimized,

$$E = \frac{\pi F(1-\nu^2)}{2\tan(\alpha)\,\delta^2}, \tag{1}$$

where F is the force exerted by the cell on the AFM cantilever, α is the half-angle opening of the square pyramid (35°), δ is the depth of probe indentation, ν is Poisson's ratio (0.5, incompressible) and E is the Young's modulus. The degree of fit of the model and the indentation range over which the model applies can be more clearly ascertained by using Eq. 1. Limited to small indentations, the elastic modulus of the cells was well described by Eq. 1. The method of Mahaffy et al. (40) was applied to

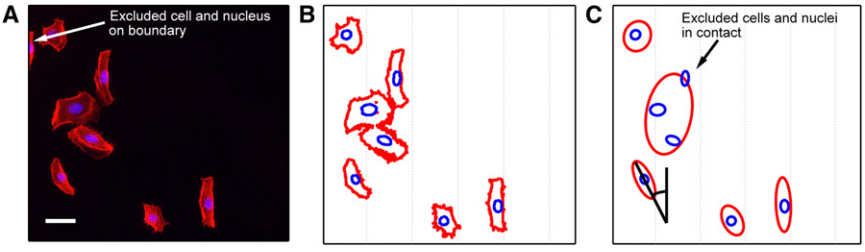

FIGURE 1 (*A*) Fluorescent image of cells on a 2000-nm topography. (*B*) Recreated boundaries of the cell cytoskeleton and nucleus from *A*. Note that the leftmost cell and its nucleus in *A* are in contact with the border of the captured image, and that cell is therefore excluded from the boundary recreation. (*C*) Generated ellipses of the recreated image. Notice that the three cells in close proximity in *A* cannot be distinguished from each other and are therefore excluded from analysis. The orientation of the ellipse in relation to the topography (running vertically) is then defined from the major axis of the ellipse, as shown for one cell. Scale bar, 40 μm.

quantitatively describe the indentation depth over which these viscoelastic cells behaved as elastic bodies. The standard deviation of Young's modulus was based on the averages from the four separate experiments. A demonstration of raw force-versus-indentation data, along with plots of Young's modulus versus indentation is shown in Fig. S1 in the Supporting Material.

RESULTS

The physical alignment of HTCEpi cells to substrate ridge and groove topography is demonstrated in Fig. 2. The image describes the relationship between the orientation of the cytoskeleton (*horizontal axis*) and nucleus (*vertical axis*) within the same cell. The upper image demonstrates cells cultured on flat surfaces and the lower image describes cells cultured on 2000-nm-pitch surfaces (largest topography). On flat surfaces, the cytoskeleton of the cell was randomly oriented between 0° and 90°, and the orientation of the nucleus was predominantly a function of cytoskeletal orientation (shown as an increased density running diagonally from lower left to upper right in Fig. 2). Although the match between cytoskeleton and nucleus orientation was not exact, the heat maps reveal a good relationship between the orientation of a cell's cytoskeleton and nucleus. They also show that cells do not have contradictory orientations of the cytoskeleton and nucleus on any pitch. On 2000-nm-pitch surfaces, both the cytoskeleton and nuclei were predominantly aligned parallel to the topography, with 26% of all cells between 0° and 10° and 47% between 0° and 20°. The net orientation (the number of cells parallel minus the number perpendicular), expressed as a percent, increased from 0% on flats to 20% parallel on a 2000-nm pitch. Heat maps and net orientation results for all the pitches are shown in Fig. 3. The net orientation of the cytoskeleton and nucleus show that not only do they align parallel with the underlying ridge and groove, but they do so with increasing preference over perpendicular alignment as the pitch increases from 400 to 2000 nm. Fig. S2 plots the mean orientation angle of the cytoskeleton and nucleus as a function of pitch with 95% confidence intervals. In a similar way, this figure describes how the cytoskeleton and nucleus preferentially align parallel with increasing frequency for increasing pitch. Based on the predominance of parallel alignment for the nucleus and cytoskeleton, we measured the elastic moduli of cells that were aligned parallel to the underlying topographies (Fig. 4).

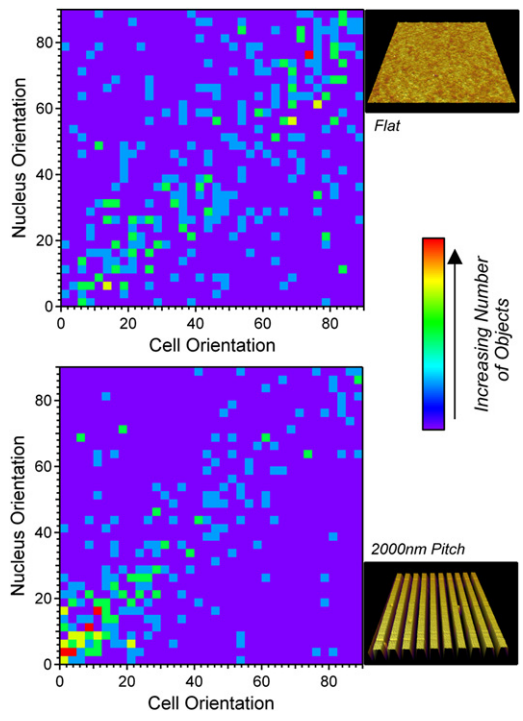

FIGURE 2 Heat maps demonstrating the relationship between the orientation of the cytoskeleton and nucleus of a cell to an underlying topography. The examples shown here were for the flat substrate (*upper*; 314 cells) and the 2000-nm-pitch substrate (*lower*; 246 cells). The topography representations were AFM height images of the actual samples rendered in 3D for visual effect (flat, area = 4 μm^2, RMS = 435 pm; 2000-nm pitch, area = 20 μm^2). Each square (2.5° L × W) on the map represents the number of objects (0 (*purple*) to 4 (*red*)) that fall within a particular orientation. Parallel and perpendicular alignment are at 0° and 90°, respectively.

The elastic modulus of aligned cells was a function of substrate topography. It is interesting to note that the modulus did not simply increase with increasing pitch size, as has been observed on nanoscale topographic islands (2) and larger 12.5-μm-pitch ridge and groove substrates (3); rather, there was a significant decrease in the cell modulus at 400 nm compared to the moduli for flat surfaces and for larger pitches of these chemically identical substrates. Chemically dissimilar ridges and grooves have been shown to alter the mechanical properties of mesenchymal stem cells (41). As the pitch increased to 800 nm and above, the elastic moduli of the cells were larger than the modulus measured on flat surfaces. Fig. 4 also shows how the mean area of the aligned nuclei varies as a function of pitch size. The similarity in trend between mean nucleus area and elastic modulus of the cell suggests that the nucleus plays an important role in the response of the cell to the applied load of the AFM cantilever. The relationship between nucleus area and elastic modulus is approximately linear (Fig. S3). Representative confocal z-stack images (Fig. 5) from 400- and 2000-nm-pitch substrates showed that the change in the nucleus shape was not limited to area but was also reflected in increasing height, indicating a change in nucleus volume. The average heights from six aligned cells on 400- and six on 2000-nm-pitch substrates were 6.7 ± 0.8 μm and 9.8 ± 1.9 μm, respectively. The internal volumes of these oriented nuclei on the 400- and 2000-nm pitches were also determined from the confocal z-stack images using image analysis features of IGOR. Fig. 6 demonstrates a 3D recreation of a confocal z-stack for an oriented nucleus on a 2000-nm topography. Using IGOR's imageseedfill operation, a 3D image of only the shell of the nucleus is generated (rotated image with green interior). A value of 1 was assigned to pixels within the shell

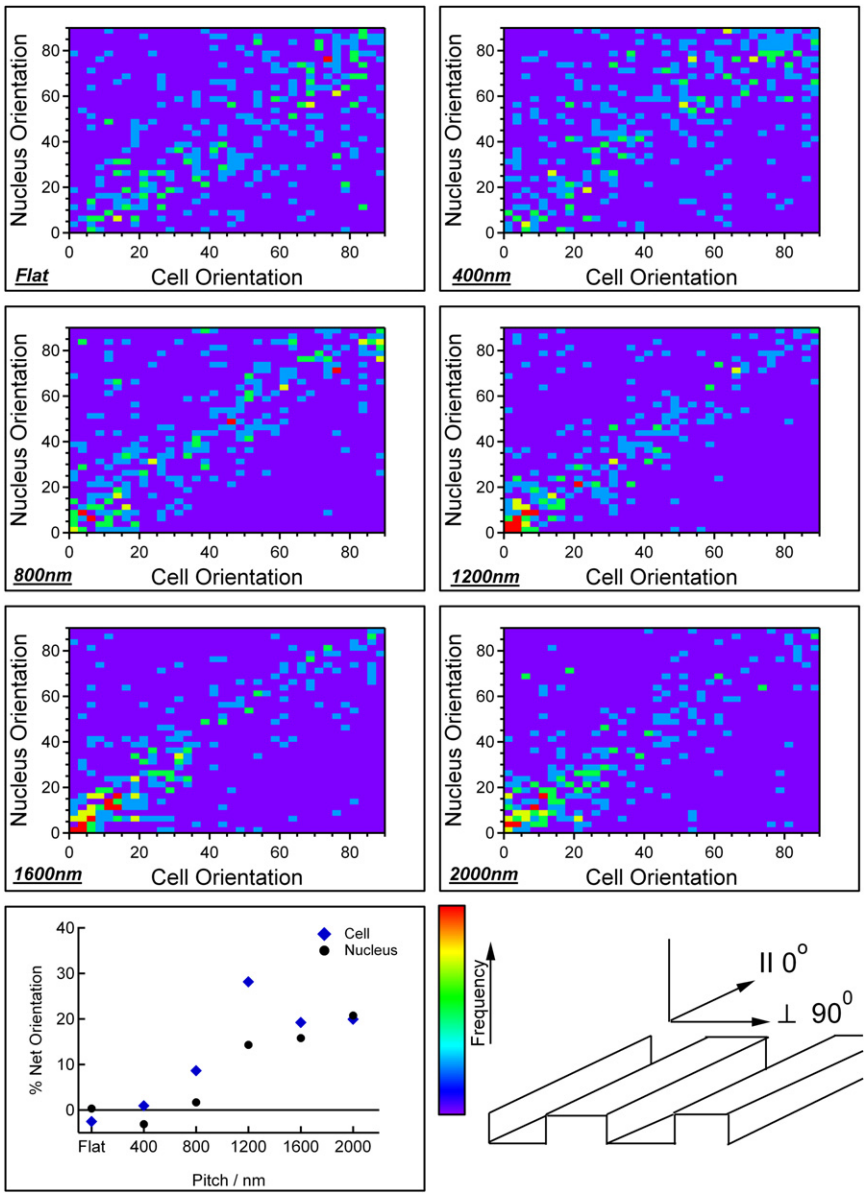

FIGURE 3 Heat maps and net orientation figures for all the pitches. Positive values of net orientation (*lower left*) represent net parallel alignment. With the exception of those at 400 nm, cells on all pitches demonstrate a net alignment response to the underlying topography. Nucleus and cell orientation are in degrees.

of the nucleus and a value of 0 to those outside the shell. The fraction occupied by the nucleus, in the total confocal volume, was determined by summing up the pixels with a value of 1 and dividing that number by the total number of pixels within the confocal volume (*dashed black box*). The volume of the nucleus was then determined by multiplying this fraction by the total volume of the confocal image (determined from x, y, and z pixel scale of image). The average volumes of the imaged nuclei on 400- and 2000-nm pitches were 787 $\pm$ 184 μm^3 and 1170 $\pm$ 331 μm^3, respectively ($p = 0.04$).

DISCUSSION

As HTECpi cells adhered to the parallel ridges and grooves, both the cytoskeleton and nucleus aligned with increasing frequency as pitch size increased. They also tended to elongate as the orientation angle approached 0° in a pitch-dependent manner, consistent with previous research from our lab on primary corneal epithelial cells (28). The orientation of the nucleus is assumed to be primarily a function of the dynamic orientation of the cytoskeleton, since cells do not maintain a fixed orientation. Confocal images did show, however, that no significant cytoplasmic volume existed between the base of the nucleus and the substrate, and in the case of the 2000-nm topography, it was observed that the nucleus deformed on its base to mimic the topography (Fig. S4). It is interesting to consider, then, that the nucleus itself can possibly be a direct mechanosensor of topography, independent of the cytoskeleton, and may therefore influence directional migration of the cell as well. Regardless of the driving mechanism for nucleus alignment, these

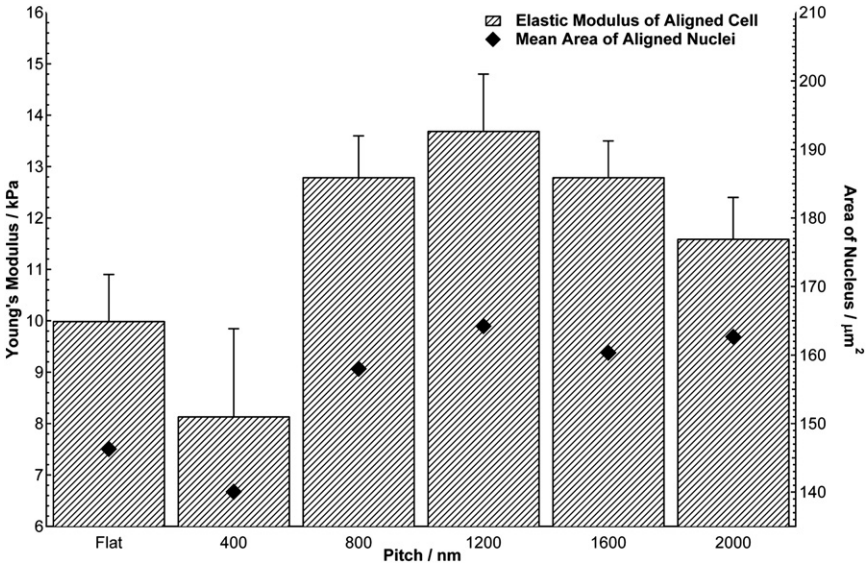

FIGURE 4 Elastic moduli of cells aligned with topography as a function of pitch (*bar graph* and *left axis*). The elastic modulus correlates well with the mean area of aligned nuclei (*black diamonds* and *right axis*). Standard deviations of nuclear mean area values were 36.7, 37.4, 35.5, 52.3, 41.3, and 43.6 μm^2 (flat to 2000-nm pitch, respectively).

results highlight the ability of a nucleus to respond to changing external biophysical cues. These data are particularly relevant given the ubiquitous presence of biophysical cues in vivo, which can change during a number of physiological events, such as with aging (42), disease (43,44), or therapeutic intervention (45).

Not only does the nucleus reorient in response to the underlying ridge and grooves, but its shape and volume are also significantly altered. Topographically driven changes in the volume of endothelial cell nuclei have been shown to influence cell proliferation rates (46), suggesting that increased nuclear volumes render DNA more accessible to replication machinery. A recent article also demonstrated the relationship between nuclear volume and cell proliferation by β-aminopropionitrile inhibition of lysyl oxidase within the nucleus (47). We have shown here that the volume of aligned nuclei was pitch-dependent, with the 400-nm topographies resulting in the smallest volume. Work from our lab (8,30) has also demonstrated that the proliferative status of vascular endothelial, corneal epithelial, and corneal fibroblast cells was significantly decreased on these 400-nm pitch ridge and groove substrates. In addition, in vascular endothelial cells, many of the genes observed to be downregulated more than twofold by contact with topographic features in the biomimetic size scale (400-nm pitch) belong to drivers of the mitotic cycle (14). Given the pitch-dependent modulation of nucleus volume for these immortalized corneal epithelial cells, we would hypothesize that change within the available volume of the nucleus leads to the previously observed changes in proliferation at 400 nm for both the corneal and vascular endothelial cells.

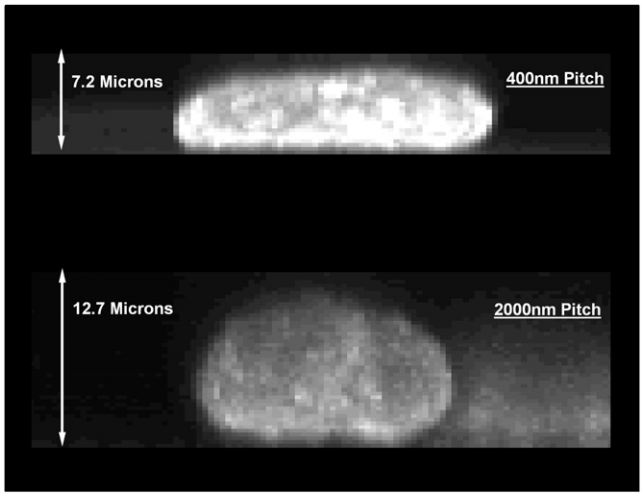

FIGURE 5 Confocal *z*-stack images of cell nuclei oriented parallel to topography on 400-nm-pitch (*upper*) and 2000-nm-pitch (*lower*) substrates. The substrates are located at the bottom of each *z*-stack.

In the course of our studies (14,28–30) with a variety of cells, we have noted that cells from different tissues can react differentially to topographically patterned substrates. Certain cells will have more pronounced gene and protein expression values on smaller-pitched substrates, whereas other cells are more influenced by larger pitches. We have noted for corneal epithelial cells that pitches in the middle range (~1200 nm) frequently exert the biggest effect on cellular behavior. A recent article sets out what is known about nuclear shape and size (48). The authors point out that shape can be altered by changes in the nuclear lamina, but because of the association of the lamina proteins with the cytoskeleton, shape can also be altered by forces exerted throughout the cytoplasmic matrix. We have previously published observations that the focal adhesions of corneal cells exhibit different orientations to parallel ridges depending on the pitch (34). The adhesions were oblique to the long axis of the ridges at the intermediate pitches tested and were parallel at the smallest and largest pitches evaluated. This observation suggests that the cytoarchitecture of the cells

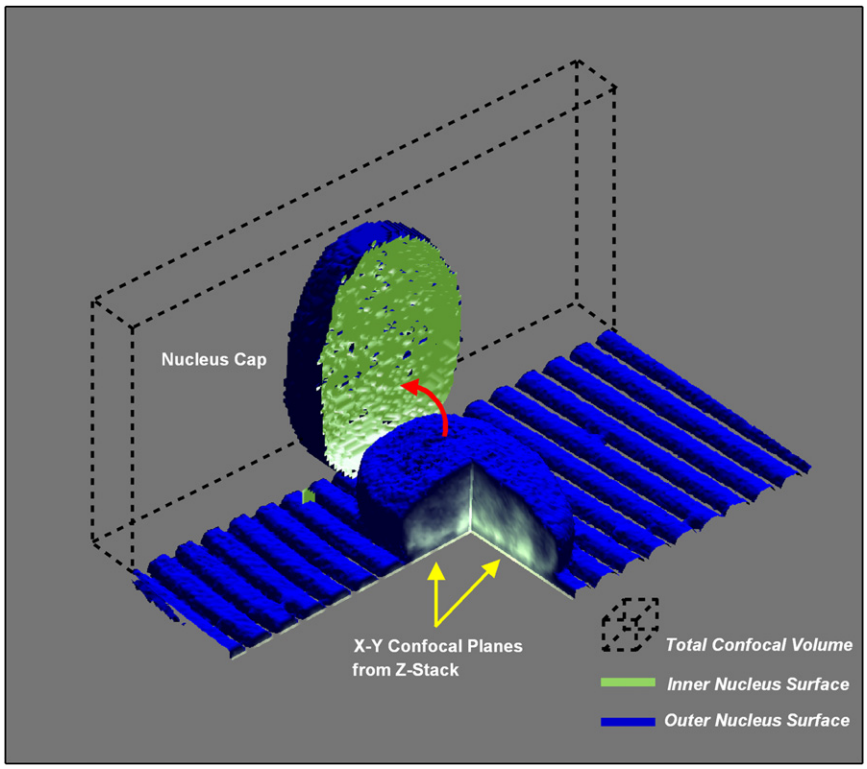

FIGURE 6 Recreation in 3D of a cell nucleus oriented on a 2000-nm-pitch topography. A portion of the 3D object has been removed so that the agreement between the confocal *z*-stack planes in the *x* and *y* directions, and the 3D rendered object, can be observed. The volume fraction occupied by the nucleus is determined by recreating the outer surface of the nucleus (cap) and then summing up the number of pixels that exist within the cap and dividing that number by the total number of pixels in the confocal volume (*dotted box*).

on the different pitches may be different and could influence cell shape. Also, it is known that changes in the levels of lamina proteins can lead to alterations in the nuclear shape (49). Gene and protein expression of lamina proteins is of interest, but the aim of the work reported here was to determine how controlled changes in the shape of the nucleus influence the interpretation of the cell elastic modulus. Factors influencing the volume of the nucleus are thought to depend on the amount of DNA in the nucleus and the extent of DNA compaction. Heterochromatin chromosomal regions that are transcriptionally inactive tend to be less open. Changes in gene expression, noted in a number of cells on differing topographies, could alter how much of the DNA is compacted. In addition, the availability of the nuclear membrane could be altered on pitch and this would influence nuclear size.

Using AFM, as well as other methods, the average mechanical properties of living cells have been studied in detail. However, given the heterogeneous and dynamic nature of living cells, it is difficult to isolate the influence of individual internal cell components on the whole-cell response to deformation. Unlike cells cultured on flat substrates or cells in suspension, these topographies influenced the shape of the nucleus in a nonrandom fashion. Variations in the elastic modulus of aligned cells could therefore be correlated with topography-dependent changes in nucleus shape. It has been shown previously that the measured elastic modulus of cells is dependent on the location at which it is measured (17), with regions over the nucleus appearing the stiffest. As mentioned, all measurements of cell modulus in this study were obtained over the central body of aligned cells where the nucleus was present. Our results demonstrate that the underlying substrate, which is on the order of 10 μm from the top of the cell, can modulate the measurement of the cell elastic modulus by altering the structural properties of the cell nucleus. As the volume of the nucleus increased, the measured cell elastic modulus increased, and we assume that this result is analogous to the previously reported (36,40) effect of the proximity of a rigid underlying substrate on measured elastic modulus. As the volume of the rigid nucleus increased in the cell (3–10 times stiffer than cell cytoplasm (26)), the resistance to deformation measured over the nuclear region increased due to the combined responses of the cell membrane, cytoskeleton, and nucleus, whose proximity to the outer dorsal membrane was decreased due to its increased volume. Conversely, the smaller the nucleus, the more cytoplasmic space exists between the nucleus and the outer cell membrane, thus offering decreased resistance to deformation by the indenting probe, as observed at the 400-nm pitch.

In conclusion, these results demonstrate that biophysical cues in the form of topographically patterned parallel ridges and grooves alter the alignment and shape of cell nuclei and cytoskeletal elements. Changes in the shape of the nucleus influence the measured elastic modulus of the cell, and we hypothesize that these changes in nuclear shape indirectly influence cell alignment and proliferation rates in a pitch-dependent manner.

SUPPORTING MATERIAL

Four figures are available at http://www.biophysj.org/biophysj/supplemental/S0006-3495(11)01133-7.

The authors acknowledge technical discussions with staff at WaveMetrics regarding 3D analyses of confocal data.

This research was funded by grants from the National Institutes of Health (R01EY016134, R01EY019475, R01EY019970, and P30EY12576) and an unrestricted grant from Research to Prevent Blindness.

REFERENCES

1. Russell, P., J. Z. Gasiorowski, …, C. J. Murphy. 2008. Response of human trabecular meshwork cells to topographic cues on the nanoscale level. *Invest. Ophthalmol. Vis. Sci.* 49:629–635.
2. Hansen, J. C., J. Y. Lim, …, H. J. Donahue. 2007. Effect of surface nanoscale topography on elastic modulus of individual osteoblastic cells as determined by atomic force microscopy. *J. Biomech.* 40:2865–2871.
3. McPhee, G., M. J. Dalby, …, H. Yin. 2010. Can common adhesion molecules and microtopography affect cellular elasticity? A combined atomic force microscopy and optical study. *Med. Biol. Eng. Comput.* 48:1043–1053.
4. McKee, C. T., J. A. Wood, …, P. Russell. 2011. The effect of biophysical attributes of the ocular trabecular meshwork associated with glaucoma on the cell response to therapeutic agents. *Biomaterials.* 32:2417–2423.
5. Isenberg, B. C., P. A. Dimilla, …, J. Y. Wong. 2009. Vascular smooth muscle cell durotaxis depends on substrate stiffness gradient strength. *Biophys. J.* 97:1313–1322.
6. Uttayarat, P., M. Chen, …, P. I. Lelkes. 2008. Microtopography and flow modulate the direction of endothelial cell migration. *Am. J. Physiol. Heart Circ. Physiol.* 294:H1027–H1035.
7. Hadjipanayi, E., V. Mudera, and R. A. Brown. 2009. Close dependence of fibroblast proliferation on collagen scaffold matrix stiffness. *J. Tissue Eng. Regen. Med.* 3:77–84.
8. Liliensiek, S. J., J. A. Wood, …, C. J. Murphy. 2010. Modulation of human vascular endothelial cell behaviors by nanotopographic cues. *Biomaterials.* 31:5418–5426.
9. Leipzig, N. D., and M. S. Shoichet. 2009. The effect of substrate stiffness on adult neural stem cell behavior. *Biomaterials.* 30:6867–6878.
10. Zinger, O., G. Zhao, …, B. Boyan. 2005. Differential regulation of osteoblasts by substrate microstructural features. *Biomaterials.* 26:1837–1847.
11. Pelham, Jr., R. J., and Y. Wang. 1997. Cell locomotion and focal adhesions are regulated by substrate flexibility. *Proc. Natl. Acad. Sci. USA.* 94:13661–13665.
12. Yim, E. K., R. M. Reano, …, K. W. Leong. 2005. Nanopattern-induced changes in morphology and motility of smooth muscle cells. *Biomaterials.* 26:5405–5413.
13. Dalby, M. J., M. O. Riehle, …, A. S. Curtis. 2003. Nucleus alignment and cell signaling in fibroblasts: response to a micro-grooved topography. *Exp. Cell Res.* 284:274–282.
14. Gasiorowski, J. Z., S. J. Liliensiek, …, C. J. Murphy. 2010. Alterations in gene expression of human vascular endothelial cells associated with nanotopographic cues. *Biomaterials.* 31:8882–8888.
15. Radmacher, M., R. W. Tillamnn, …, H. E. Gaub. 1992. From molecules to cells: imaging soft samples with the atomic force microscope. *Science.* 257:1900–1905.
16. Martens, J. C., and M. Radmacher. 2008. Softening of the actin cytoskeleton by inhibition of myosin II. *Pflugers Arch.* 456:95–100.
17. Mathur, A. B., G. A. Truskey, and W. M. Reichert. 2000. Atomic force and total internal reflection fluorescence microscopy for the study of force transmission in endothelial cells. *Biophys. J.* 78:1725–1735.
18. Hofmann, U. G., C. Rotsch, …, M. Radmacher. 1997. Investigating the cytoskeleton of chicken cardiocytes with the atomic force microscope. *J. Struct. Biol.* 119:84–91.
19. Guilak, F. 1995. Compression-induced changes in the shape and volume of the chondrocyte nucleus. *J. Biomech.* 28:1529–1541.
20. Caille, N., Y. Tardy, and J. J. Meister. 1998. Assessment of strain field in endothelial cells subjected to uniaxial deformation of their substrate. *Ann. Biomed. Eng.* 26:409–416.
21. Sims, J. R., S. Karp, and D. E. Ingber. 1992. Altering the cellular mechanical force balance results in integrated changes in cell, cytoskeletal and nuclear shape. *J. Cell Sci.* 103:1215–1222.
22. Ingber, D. E. 2003. Tensegrity I. Cell structure and hierarchical systems biology. *J. Cell Sci.* 116:1157–1173.
23. Chancellor, T. J., J. Lee, …, T. Lele. 2010. Actomyosin tension exerted on the nucleus through nesprin-1 connections influences endothelial cell adhesion, migration, and cyclic strain-induced reorientation. *Biophys. J.* 99:115–123.
24. Starr, D. A., and M. Han. 2002. Role of ANC-1 in tethering nuclei to the actin cytoskeleton. *Science.* 298:406–409.
25. Kuznetsova, T. G., M. N. Starodubtseva, …, R. I. Zhdanov. 2007. Atomic force microscopy probing of cell elasticity. *Micron.* 38: 824–833.
26. Lammerding, J., K. N. Dahl, …, R. D. Kamm. 2007. Nuclear mechanics and methods. *Methods Cell Biol.* 83:269–294.
27. Hochmuth, R. M. 2000. Micropipette aspiration of living cells. *J. Biomech.* 33:15–22.
28. Teixeira, A. I., G. A. Abrams, …, P. F. Nealey. 2003. Epithelial contact guidance on well-defined micro- and nanostructured substrates. *J. Cell Sci.* 116:1881–1892.
29. Reference deleted in proof.
30. Liliensiek, S. J., S. Campbell, …, C. J. Murphy. 2006. The scale of substratum topographic features modulates proliferation of corneal epithelial cells and corneal fibroblasts. *J. Biomed. Mater. Res. A.* 79:185–192.
31. Rotsch, C., and M. Radmacher. 2000. Drug-induced changes of cytoskeletal structure and mechanics in fibroblasts: an atomic force microscopy study. *Biophys. J.* 78:520–535.
32. Zhang, Q., C. Ragnauth, …, R. G. Roberts. 2002. The nesprins are giant actin-binding proteins, orthologous to *Drosophila melanogaster* muscle protein MSP-300. *Genomics.* 80:473–481.
33. Karuri, N. W., S. Liliensiek, …, C. J. Murphy. 2004. Biological length scale topography enhances cell-substratum adhesion of human corneal epithelial cells. *J. Cell Sci.* 117:3153–3164.
34. Teixeira, A. I., G. A. McKie, …, C. J. Murphy. 2006. The effect of environmental factors on the response of human corneal epithelial cells to nanoscale substrate topography. *Biomaterials.* 27:3945–3954.
35. Robertson, D. M., L. Li, …, J. V. Jester. 2005. Characterization of growth and differentiation in a telomerase-immortalized human corneal epithelial cell line. *Invest. Ophthalmol. Vis. Sci.* 46:470–478.
36. Radmacher, M., M. Fritz, …, P. K. Hansma. 1996. Measuring the viscoelastic properties of human platelets with the atomic force microscope. *Biophys. J.* 70:556–567.
37. Radmacher, M. 2007. Studying the mechanics of cellular processes by atomic force microscopy. *Methods Cell Biol.* 83:347–372.
38. Hutter, J. L., and J. Bechhoefer. 1993. Calibration of atomic force microscope tips. *Rev. Sci. Instrum.* 64:1868–1873, erratum 64:3342.
39. Love, A. E. H. 1939. Boussinesq's problem for a rigid cone. *Q. J. Math.* 10:161–175.
40. Mahaffy, R. E., C. K. Shih, …, J. Käs. 2000. Scanning probe-based frequency-dependent microrheology of polymer gels and biological cells. *Phys. Rev. Lett.* 85:880–883.

41. Yim, E. K., E. M. Darling, …, K. W. Leong. 2010. Nanotopography-induced changes in focal adhesions, cytoskeletal organization, and mechanical properties of human mesenchymal stem cells. *Biomaterials.* 31:1299–1306.

42. Truscott, R. J. 2009. Presbyopia. Emerging from a blur towards an understanding of the molecular basis for this most common eye condition. *Exp. Eye Res.* 88:241–247.

43. Last, J. A., T. Pan, …, P. Russell. 2011. Elastic modulus determination of normal and glaucomatous human trabecular meshwork. *Invest. Ophthalmol. Vis. Sci.* 52:2147–2152.

44. Matsumoto, T., H. Abe, …, M. Sato. 2002. Local elastic modulus of atherosclerotic lesions of rabbit thoracic aortas measured by pipette aspiration method. *Physiol. Meas.* 23:635–648.

45. Kymionis, G., and D. Portaliou. 2007. Corneal crosslinking with riboflavin and UVA for the treatment of keratoconus. *J. Cataract Refract. Surg.* 33:1143–1144, author reply 1144.

46. Roca-Cusachs, P., J. Alcaraz, …, D. Navajas. 2008. Micropatterning of single endothelial cell shape reveals a tight coupling between nuclear volume in G1 and proliferation. *Biophys. J.* 94:4984–4995.

47. Saad, F. A., M. Torres, …, L. Graham. 2010. Intracellular lysyl oxidase: effect of a specific inhibitor on nuclear mass in proliferating cells. *Biochem. Biophys. Res. Commun.* 396:944–949.

48. Webster, M., K. L. Witkin, and O. Cohen-Fix. 2009. Sizing up the nucleus: nuclear shape, size and nuclear-envelope assembly. *J. Cell Sci.* 122:1477–1486.

49. Dahl, K. N., A. J. S. Ribeiro, and J. Lammerding. 2008. Nuclear shape, mechanics, and mechanotransduction. *Circ. Res.* 102:1307–1318.